[Chem. Pharm. Bull. 34(9)3779—3790(1986)]

Degradation Kinetics of Carumonam in Aqueous Solution

YOSHIO MATSUHISA,* KAZUICHI UMEMOTO, KOICHI ITAKURA, and YOSHIRO USUI

Chemical Development Laboratories, Central Research Division, Takeda Chemical Industries, Ltd., Yodogawa-ku, Osaka 532, Japan

(Received March 6, 1986)

The degradation and kinetics of carumonam (**1**) in aqueous solution were investigated by high-performance liquid chromatography (HPLC) at 35 °C and an ionic strength of 0.5 over the pH range of 0 to 10. All the main degradation products observed by HPLC were isolated and identified. It was concluded that these products were formed by a combination of five reactions, a β-lactam ring-opening reaction, reversible C_3-epimerization, reversible *syn–anti* isomerization, desulfonation, and a decarbamoylation reaction. The overall rate of degradation was of pseudo-first-order type and was influenced by solvolytic, hydrogen ion, and hydroxide ion catalysis. Simultaneous reversible C_3-epimerization and β-lactam ring-opening reaction, which occur in neutral and alkaline solutions, proved to be catalyzed by hydroxide ion. The pH-rate profile for **1** exhibited a unique W-shape due to *syn–anti* isomerization in a specific pH region. The maximum stability of **1** was observed in the pH range of 4.9 to 5.8. The theoretical pH-rate profile agreed well with the experimental data, and primary salt effect was also considered theoretically. The activation energies determined at $\mu = 0.5$ were 22.3, 15.6 and 17.5 kcal/mol at pH 4.40, 7.01 and 8.88, respectively.

Keywords——carumonam; sulfazecin; monocyclic β-lactam antibiotic; kinetics; stability; degradation; dissociation constant; HPLC

Introduction

A novel monocyclic β-lactam antibiotic, sulfazecin, was recently discovered in a bacterial culture and its unique structure with a 1-sulfo-3-azetidinone moiety was elucidated by Imada *et al.*[1] Many derivatives were synthesized by Kishimoto *et al.*[2] This paper describes the degradation and epimerization kinetics of a derivative, (*Z*)-[[[1-(2-amino-4-thiazolyl)-2-[[(2*S*,3*S*)-2-(carbamoyloxymethyl)-4-oxo-1-sulfo-3-azetidinyl]amino]-2-oxoethylidene]amino]oxy]acetic acid (**1**, carumonam),[2b] which is more effective against gram-negative bacteria than sulfazecin.

Experimental

Materials——The disodium salt of **1**, carumonam sodium, used in this study was synthesized in our Division. All other chemicals used were of the highest commercial grade available.

Disodium Salt of **1**: *Anal.* Calcd for $C_{12}H_{12}N_6Na_2O_{10}S_2 \cdot 0.5H_2O$: C, 27.75; H, 2.52; N, 16.18; S, 12.35. Found: C, 27.78; H, 2.57; N, 16.14; S, 12.21. $[\alpha]_D^{20}$ ($c=1$, H_2O): +19.9°. UV $\lambda_{max}^{H_2O}$ nm ($E_{1\,cm}^{1\%}$): 231 (235), 295 (134). IR ν_{max}^{KBr} cm^{-1}: 3463, 3432, 3358, 3292, 1780, 1713, 1649, 1618, 1417, 1060. NMR (10% solution, D_2O) δ: 4.3—4.5 (2H, m, $-CH_2OCONH_2$), 4.55 (2H, s, $-CH_2COONa$), 4.62 (1H, m, C_2-H), 5.55 (1H, d, $J=5.6$ Hz, C_3-H), 7.00 (1H, s, C_5-H on aminothiazole).

Buffer Solutions——The buffer systems used in the kinetic study were hydrochloric acid (pH 0.0), hydrochloric acid–potassium chloride (pH 1.06, 1.34, 1.91), citrate buffer (pH 2.59, 2.75, 3.04), acetate buffer (pH 3.85, 4.08, 4.40, 4.90), phosphate buffer (pH 5.84, 7.01, 7.82), and borate buffer (pH 7.92, 8.88, 9.12, 9.50, 9.57, 9.96, 9.99). The buffers were 0.1 M with respect to citrate, acetate, phosphate and borate ions except when the catalytic salt effects were studied. The buffers were adjusted to an ionic strength (μ) of 0.5 with sodium chloride, except when the primary salt effects were studied. The pH of each solution was measured at the experimental temperature both at the beginning

and at the end of experiments using a pH meter equipped with a combination electrode. No significant changes in pH were observed.

Analytical Procedure——The residual **1** and its degradation products were determined by high-performance liquid chromatography (HPLC) using a reversed-phase column. The HPLC system was equipped with a solvent delivery system (Waters Assoc., model 6000 A) and a ultraviolet (UV) detector set at 254 nm (Waters Assoc., model 440). A stainless steel column (15 × 0.4 cm i.d.) was packed with octadecylsilane chemically bonded on silica gel (Nucleosil® $5C_{18}$, Macherey Nagel Co.) and protected by a precolumn (1 × 0.4 cm i.d.) with the same filler. To separate **1** and its degradation products, a mixture of 0.01% ammonium sulfate, methanol and glacial acetic acid (97 : 2 : 1, v/v) was used as the mobile phase. The flow rate was 0.8 ml/min at the controlled room temperature and the injection volume was 20 μl. The peak areas were integrated with a Hewlett-Packard HP 3357 and converted to molar fractions.

Kinetic Procedure——In most cases, the kinetic studies were carried out at 35 °C. Approximately 50 mg of disodium salt of **1** was accurately weighed and dissolved in 50 ml of appropriate buffer to make a sample solution of 2.0×10^{-3} M. All buffers were preheated to the temperature of the study. The sample solutions were sealed and stored in a constant temperature bath which was regulated by a thermostat with ±0.1 °C precision. Aliquots of 2 ml were withdrawn at the desired time intervals, and immediately diluted to 10 ml with the mobile phase of HPLC and analyzed.

pK_a Determination——The mixed pK_a values[3] of **1** at 35 °C and μ=0.2, 0.5 and 0.8 (adjusted with sodium chloride) were determined by the potentiometric titration method. About 8.0×10^{-3} M disodium salt of **1** was titrated with 0.1 N HCl under nitrogen and changes of pH were measured with an autotitration pH meter (Radiometer Co., RTS822 titration recording system).

Isolation of Degradation Products——All the main degradation products detected by HPLC were isolated and purified using a preparative reversed-phase HPLC column (YMC SH-343 25 × 2 cm i.d., Yamamura Chemical Laboratory Co., Ltd.), XAD-2 column (200—400 mesh, 50 × 3 cm i.d.) or Sephadex G-25 column (20—80 μm, 95 × 3 cm i.d.) with a UV detector set at 254 nm. The purity of these isolated compounds was determined by analytical HPLC under the conditions described in the analytical procedure. The structures were mainly characterized or identified by spectroscopy.

(*Z*)-[[[1-(2-Amino-4-thiazolyl)-2-[[(1*S*,2*S*)-3-carbamoyloxy-1-carboxy-2-sulfoaminopropyl]amino]-2-oxoethylidene]amino]oxy]acetic Acid (**2**): The disodium salt of **1**, 4 g, was dissolved in 60 ml of water and the pH was adjusted to pH 12.0 with 1 N NaOH. This solution was kept for 4 h at 70 °C, then neutralized to pH 6.7 with 2 N HCl before lyophilization. Compound **2** was isolated and purified using an XAD-2 column with a flow rate of water of 2.5 ml/min. The purity of **2** (yield 370 mg) was estimated to be 98.0% on the basis of the peak-area ratio.

Anal. Calcd for $C_{12}H_{16}N_6O_{11}S_2 \cdot 1.5H_2O$: C, 28.18; H, 3.74; N, 16.43; S, 12.54. Found: C, 28.45; H, 3.88; N, 16.23; S, 12.66. $[\alpha]_D^{20}$ (c=0.1, H_2O, pH 6.8): −4.8°. UV $\lambda_{max}^{H_2O\,(pH\,6.8)}$ nm ($E_{1\,cm}^{1\%}$): 234 (226), 292 (138). IR ν_{max}^{KBr} cm^{-1}: 1726, 1633, 1039. NMR (10% solution, D_2O) δ: 4.0—4.4 (3H, m, $-C\underline{H}_2OCONH_2$ and $-C\underline{H}(NHSO_3H)-$), 4.84 (1H, d, J=3.0 Hz, $-CONHC\underline{H}(COOH)-$), 7.23 (1H, s, C_5-$\underline{H}$ on aminothiazole).

(*Z*)-[[[1-(2-Amino-4-thiazolyl)-2-[[(2*S*,3*R*)-2-(carbamoyloxymethyl)-4-oxo-1-sulfo-3-azetidinyl]amino]-2-oxoethylidene]amino]oxy]acetic Acid (**3**): The disodium salt of **1**, 5 g, was dissolved in 500 ml of 0.2 M phosphate buffer (pH 10.0), and the solution was kept for 0.5 h at 40 °C, then neutralized to pH 6.0 with glacial acetic acid before lyophilization. Compound **3** was isolated by preparative reversed-phase HPLC with a mobile phase of 0.1% sodium carbonate, methanol and glacial acetic acid (100 : 1 : 1, v/v) and then desalted with a mobile phase of water, acetonitrile and glacial acetic acid (100 : 1 : 1, v/v). In both cases, the flow rate was 10 ml/min. The purity of **3** (yield 70 mg) was estimated as described for **2** and was found to be 96.0%.

Anal. Calcd for $C_{12}H_{14}N_6O_{10}S_2 \cdot 2.0H_2O$: C, 28.69; H, 3.61; N, 16.73; S, 12.76. Found: C, 28.72; H, 3.33; N, 16.79; S, 12.51. $[\alpha]_D^{20}$ (c=0.1, H_2O, pH 6.8): +41.2°. UV $\lambda_{max}^{H_2O\,(pH\,6.8)}$ nm ($E_{1\,cm}^{1\%}$): 232 (254), 294 (145). IR ν_{max}^{KBr} cm^{-1}: 1767, 1721, 1632, 1047. NMR (DMSO-d_6) δ: 3.8—4.3 (3H, m, $-C\underline{H}_2OCONH_2$ and C_2-$\underline{H}$), 4.71 (2H, s, $-C\underline{H}_2COOH$), 4.84 (1H, dd, J=8.4, 2.4 Hz, C_3-$\underline{H}$), 7.03 (1H, s, C_5-$\underline{H}$ on aminothiazole), 9.53 (1H, d, J=8.4 Hz, $-CON\underline{H}-$).

(*Z*)-[[[1-(2-Amino-4-thiazolyl)-2-[[(1*R*,2*S*)-3-carbamoyloxy-1-carboxy-2-sulfoaminopropyl]amino]-2-oxoethylidene]amino]oxy]acetic Acid (**4**): The disodium salt of **1**, 3 g, was dissolved in 200 ml of 0.2 M carbonate buffer (pH 10.0), and the solution was kept for 7 h at 35 °C, then neutralized to pH 5.0 with 1 N HCl before lyophilization. Compound **4** was isolated with the preparative reversed-phase HPLC column with a mobile phase of water, glacial acetic acid and acetonitrile (1000 : 10 : 3, v/v) flowing at 10 ml/min. The purity of **4** (yield 31 mg) was estimated as described for **2** and was found to be 97.4%.

Anal. Calcd for $C_{12}H_{16}N_6O_{11}S_2 \cdot 2.5H_2O$: C, 27.22; H, 4.00; N, 15.87; S, 12.11. Found: C, 27.22; H, 3.62; N, 15.56; S, 12.31. $[\alpha]_D^{20}$ (c=0.1, H_2O, pH 6.8): +5.6°. UV $\lambda_{max}^{H_2O\,(pH\,6.8)}$ nm ($E_{1\,cm}^{1\%}$): 235 (226), 293 (128). IR ν_{max}^{KBr} cm^{-1}: 1725, 1635, 1035. NMR (10% solution, D_2O) δ: 4.0—4.4 (3H, m, $-C\underline{H}_2OCONH_2$ and $-C\underline{H}(NHSO_3H)-$), 4.86 (2H, s, $-C\underline{H}_2COOH$), 4.98 (1H, d, J=4.2 Hz, $-CONHC\underline{H}(COOH)-$), 7.21 (1H, s, C_5-$\underline{H}$ on aminothiazole).

(*Z*)-[[[1-(2-Amino-4-thiazolyl)-2-[[(1*S*,2*S*)-1-carboxy-3-hydroxy-2-sulfoaminopropyl]amino]-2-oxoethylidene]amino]oxy]acetic Acid (**5**) and (*Z*)-[[[1-(2-Amino-4-thiazolyl)-2-[[(1*R*,2*S*)-1-carboxy-3-hydroxy-2-sulfoaminopropyl]amino]-2-oxoethylidene]amino]oxy]acetic Acid (**6**): The disodium salt of **1**, 1 g, was dissolved in 15 ml of 1 N NaOH,

and the solution was kept for 2 h at 60 °C, then lyophilized. The target compounds were isolated and purified using the preparative reversed-phase HPLC column with a mixture of water and glacial acetic acid (200 : 1, v/v) as the mobile phase. The flow rate was 10 ml/min. The purities of both **5** (yield 12.9 mg) and **6** (yield 6 mg) were estimated as described for **2** and were found to be 95.1%. Compounds **4** and **5** were eluted overlapping as a single peak under the HPLC conditions described for the analytical procedure. They were separated by HPLC with a mobile phase of 0.005 M tetra-*n*-butylammonium bromide, methanol and formic acid (97 : 2 : 1, v/v).

Compound **5**: *Anal.* Calcd for $C_{11}H_{15}N_5O_{10}S_2 \cdot 1.6H_2O$: C, 28.10; H, 3.90; N, 14.89. Found: C, 28.07; H, 3.81; N, 14.79. $[\alpha]_D^{20}$ ($c=0.1$, H_2O, pH 6.8): $-5.9°$. UV $\lambda_{max}^{H_2O\,(pH\,6.8)}$ nm ($E_{1\,cm}^{1\%}$): 234 (256), 292 (155). IR ν_{max}^{KBr} cm^{-1}: 1726, 1635, 1037. NMR (10% solution, D_2O) δ: 3.5—4.2 (3H, m, $-CH_2OH$ and $-CH(NHSO_3H)-$), 4.86 (2H, s, $-CH_2COOH$), 4.96 (1H, d, $J=3.9$ Hz, $-CH(COOH)-$), 7.22 (1H, s, C_5-H on aminothiazole).

Compound **6**: *Anal.* Calcd for $C_{11}H_{15}N_5O_{10}S_2 \cdot 2.5H_2O$: C, 27.16; H, 4.14; N, 14.40. Found: C, 27.07; H, 3.91; N, 14.22. $[\alpha]_D^{22}$ ($c=0.1$, H_2O, pH 6.8): $+15.2°$. UV $\lambda_{max}^{H_2O\,(pH\,6.8)}$ nm ($E_{1\,cm}^{1\%}$): 234 (232), 292 (136). IR ν_{max}^{KBr} cm^{-1}: 1729, 1633, 1033. NMR (10% solution, D_2O) δ: 3.6—4.0 (3H, m, $-CH_2OH$ and $-CH(NHSO_3H)-$), 4.82 (2H, s, $-CH_2COOH$), 5.00 (1H, d, $J=3.3$ Hz, $-CH(COOH)-$), 7.23 (1H, s, C_5-H on aminothiazole).

(*E*)-[[[1-(2-Amino-4-thiazolyl)-2-[[(2*S*,3*S*)-2-(carbamoyloxymethyl)-4-oxo-1-sulfo-3-azetidinyl]amino]-2-oxoethylidene]amino]oxy]acetic Acid (**7**): The disodium salt of **1**, 3.5 g, was dissolved in 200 ml of 0.2 M citrate buffer (pH 3.0), and the solution was kept for one month at *ca.* 25 °C, then lyophilized. Compound **7** was isolated and purified using the preparative reversed-phase HPLC column with a mobile phase of water, acetonitrile and glacial acetic acid (100 : 5 : 1, v/v) flowing at 10 ml/min. The purity of **7** (yield 172 mg) was estimated as described for **2** and was found to be 98.9%.

Anal. Calcd for $C_{12}H_{14}N_6O_{10}S_2 \cdot 2.5H_2O$: C, 28.18; H, 3.74; N, 16.43; S, 12.54. Found: C, 28.42; H, 3.57; N, 16.33; S, 12.44. $[\alpha]_D^{20}$ ($c=0.1$, H_2O, pH 6.8): $+29.2°$. UV $\lambda_{max}^{H_2O\,(pH\,6.8)}$ nm ($E_{1\,cm}^{1\%}$): 233 (308), 300 (63). IR ν_{max}^{KBr} cm^{-1}: 1758, 1703, 1633, 1054. NMR (DMSO-d_6) δ: 4.0—4.3 (3H, m, $-CH_2OCONH_2$ and C_2-H), 4.93 (2H, s, $-CH_2COOH$), 5.22 (1H, dd, $J=5$, 9.0 Hz, C_3-H), 7.92 (1H, s, C_5-H on aminothiazole), 9.27 (1H, d, $J=9.0$ Hz, $-CONH-$).

(*Z*)-[[[1-(2-Amino-4-thiazolyl)-2-[[(2*S*,3*S*)-2-(carbamoyloxymethyl)-4-oxo-3-azetidinyl]amino]-2-oxoethylidene]amino]oxy]acetic Acid (**8**), (*E*)-[[[1-(2-Amino-4-thiazolyl)-2-[[(1*S*,2*S*)-3-carbamoyloxy-1-carboxy-2-sulfoaminopropyl]amino]-2-oxoethylidene]amino]oxy]acetic Acid (**9**) and (*Z*)-[[[1-(2-Amino-4-thiazolyl)-2-[[(1*S*,2*S*)-2-amino-3-carbamoyloxy-1-carboxypropyl]amino]-2-oxoethylidene]amino]oxy]acetic Acid (**10**): The disodium salt of **1**, 5 g, was dissolved in 1000 ml of 0.1 N HCl, and the solution was kept for 48 h at 60 °C, then lyophilized. The target compounds were isolated using a Sephadex G-25 column with 0.2% sodium chloride flowing at 1.5 ml/min, and were purified using the preparative reversed-phase HPLC column with 1% acetic acid flowing at 2.0 ml/min. The purities of **8** (yield 60 mg), **9** (yield 31 mg) and **10** (yield 41 mg) were estimated as described for **2** and were found to be 99.0%, 97.4% and 97.8%, respectively.

Compound **8**: *Anal.* Calcd for $C_{12}H_{14}N_6O_7S \cdot 1.7H_2O$: C, 34.57; H, 4.21; N, 20.15; S, 7.69. Found: C, 34.74; H, 4.05; N, 19.95; S, 7.69. $[\alpha]_D^{20}$ ($c=0.1$, H_2O, pH 6.8): $+28.2°$. UV $\lambda_{max}^{H_2O\,(pH\,6.8)}$ nm ($E_{1\,cm}^{1\%}$): 232 (283), 295 (163). IR ν_{max}^{KBr} cm^{-1}: 1746, 1715, 1632. NMR (DMSO-d_6) δ: 3.8—4.3 (3H, m, $-CH_2OCONH_2$ and C_2-H), 4.56 (2H, s, $-CH_2COOH$), 5.23 (1H, dd, $J=8.8$, 4.0 Hz, C_3-H), 6.74 (1H, s, C_5-H on aminothiazole), 8.40 (1H, $-NH-$ on β-lactam ring), 9.10 (1H, d, $J=8.8$ Hz, $-CONH-$).

Compound **9**: *Anal.* Calcd for $C_{12}H_{16}N_6O_{11}S_2 \cdot 2.5H_2O$: C, 27.22; H, 4.00; N, 15.87; S, 12.11. Found: C, 27.18; H, 3.75; N, 15.71; S, 11.97. $[\alpha]_D^{22}$ ($c=0.1$, H_2O, pH 6.8): $+7.8°$. UV $\lambda_{max}^{H_2O\,(pH\,6.8)}$ nm ($E_{1\,cm}^{1\%}$): 234 (289), 300 (65). IR ν_{max}^{KBr} cm^{-1}: 1722, 1632, 1040. NMR (10% solution, D_2O) δ: 4.0—4.3 (3H, m, $-CH_2OCONH_2$ and $-CH(NHSO_3H)-$), 4.79 (2H, s, $-CH_2COOH$), 7.75 (1H, s, C_5-H on aminothiazole).

Compound **10**: *Anal.* Calcd for $C_{12}H_{16}N_6O_8S \cdot 2.4H_2O$: C, 32.20; H, 4.68; N, 18.78; S, 7.16. Found: C, 32.37; H, 4.35; N, 18.52; S, 7.35. $[\alpha]_D^{20}$ ($c=0.1$, H_2O, pH 6.8): $-1.9°$. UV $\lambda_{max}^{H_2O\,(pH\,6.8)}$ nm ($E_{1\,cm}^{1\%}$): 234 (265), 294 (157). IR ν_{max}^{KBr} cm^{-1}: 1720, 1623. NMR (DMSO-d_6) δ: 3.6—4.2 (3H, m, $-CH_2OCONH_2$ and $-CH(NHSO_3H)-$), 4.51 (2H, s, $-CH_2COOH$), 6.91 (1H, s, C_5-H on aminothiazole), 8.28 (1H, d, $J=4.5$ Hz, $-CONH-$).

Results and Discussion

Degradation Pathway

Typical chromatograms of the degraded samples of **1** in acidic (pH 1.06) and alkaline (pH 9.50) solutions, together with the initial sample solution of **1**, are shown in Fig. 1.

In the neutral to alkaline pH region, **2** (β-lactam ring-opening product of **1**) and **3** (*R*-epimer of **1**) were formed from **1** by two parallel reactions of β-lactam ring opening and epimerization at the C-3 position of **1**, respectively. Compound **4** was also formed from **3** by β-lactam ring opening. Reversible epimerization was observed between **1** and **3**, but not between **2** and **4**. Only these four compounds were observed and the total molar fractions of

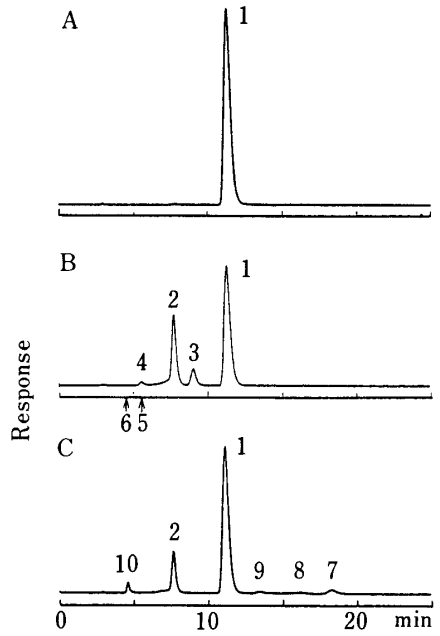

Fig. 1. Chromatograms of Degraded Samples of **1** in Acidic and Alkaline Solutions

A, initial sample solution; B, degraded sample in alkaline solution (pH 9.50, $\mu=0.5$) at 35 °C for 0.8 h (residual content of **1**: 61.3%); C, degraded sample in acidic solution (pH 1.06, $\mu=0.5$) at 35 °C for 340 h (residual content of **1**: 74.2%); 1, **1**; 2, **2**; 3, **3**; 4, **4**; ←5, the retention time of **5**; ←6, the retention time of **6**; 7, **7**; 8, **8**; 9, **9**; 10, **10**.

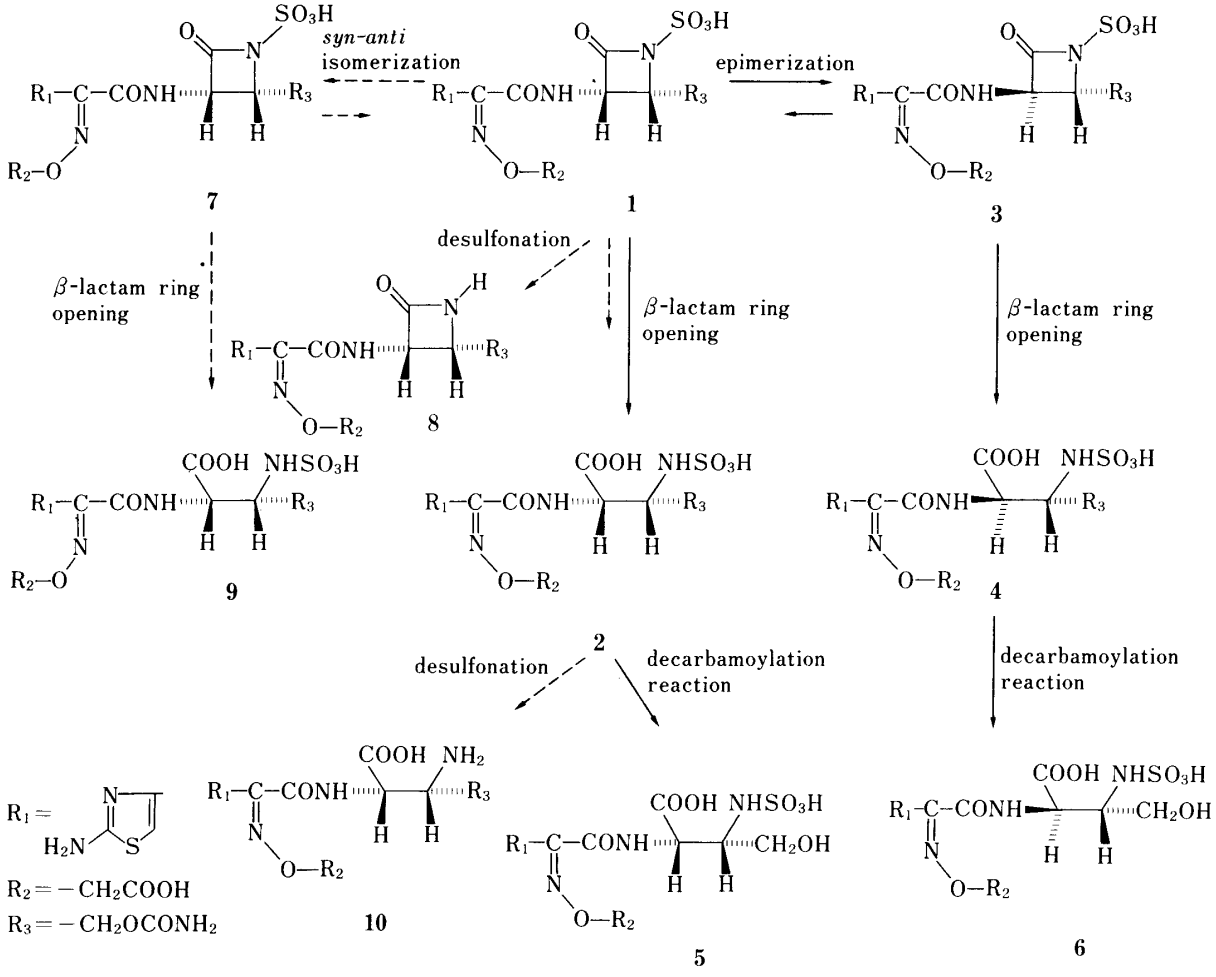

Chart 1

these compounds were the same as that of the initial solutions during the degradation. In neutral solution, only negligible amounts of **3** and **4** were formed. In more alkaline solution, **1** decomposed rapidly to **2** and **4** and the decarbamoylation reaction was also observed with respect to **2** and **4** to afford **5** and **6**, respectively.

In acidic solution, **2** and **7** (*E*-isomer of **1**) were mainly formed by the two reactions of β-lactam ring opening and *syn–anti* isomerization at the methoxyimino moiety, with trace amounts of **8** (desulfonylation product of **1**) and **9** (β-lactam ring-opening product of **7**). *syn–anti* isomerization of **1** occurred mostly around pH 3 to afford **7**, and the maximum reaction rate was observed at this pH range. Reversible *syn–anti* isomerization was observed between **1** and **7**. In strongly acidic solution, desulfonation of **2** affording **10** was also observed.

These results show that the degradation products of **1** in aqueous solution were formed by a combination of five reactions, a β-lactam ring-opening reaction, reversible C_3-epimerization, reversible *syn–anti* isomerization, desulfonation and a decarbamoylation reaction. The proposed degradation pathway of **1** in aqueous solution is shown in Chart 1.

Reaction Order and Rate

The degradation of **1** followed pseudo-first-order kinetics at constant pH, temperature and ionic strength over the pH range investigated. Reasonable linear plots of the logarithmic value of concentration *versus* time were obtained at 35 °C and other temperatures studied. Figure 2 shows the time course of degradation of **1** at several pH values at 35 °C and $\mu=0.5$, and Table I gives the observed rate constants together with the buffer systems employed in the

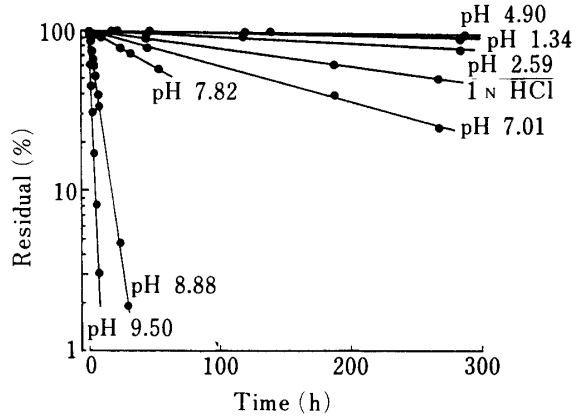

Fig. 2. Time Courses for Degradation of **1** in Buffer Solutions of Various pH Values at 35 °C and $\mu=0.5$

TABLE I. Observed Pseudo-First-Order Rate Constants for Degradation of **1** in Various Buffer Solutions at 35 °C and $\mu=0.5$

pH	Buffer system	$k_{obs}\times10^4$ (h^{-1})	pH	Buffer system	$k_{obs}\times10^4$ (h^{-1})
0	HCl	50.6	5.84	Phosphate	3.3[a]
1.06	HCl–KCl	7.9	7.01	Phosphate	20.9[a]
1.34	HCl–KCl	5.8	7.82	Phosphate	105[a]
1.91	HCl–KCl	8.1	7.92	Borate	132[a]
2.59	Citrate	11.9	8.88	Borate	1370
2.75	Citrate	12.3	9.12	Borate	2010[a]
3.04	Citrate	11.1	9.50	Borate	4570[a]
3.85	Acetate	7.0	9.57	Borate	6120
4.08	Acetate	5.3	9.96	Borate	13900
4.40	Acetate	4.1	9.99	Borate	12700[a]
4.90	Acetate	3.2			

a) Rate constants obtained by extrapolation to zero buffer concentration.

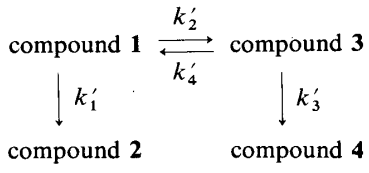

Chart 2

kinetic study.

Reversible epimerization at the C-3 position of **1** was observed. Chart 2 shows the degradation pathway in alkaline and neutral solutions, where k_1', k_2', k_3', and k_4' correspond to the rate constants of β-lactam ring opening of **1**, epimerization of **1**, β-lactam ring opening of **3** and epimerization of **3**, respectively. The following differential equations (Eqs. 1 to 4) are based on Chart 2.

$$dc_1/dt = -(k_1'+k_2')c_1 + k_4'c_3 \quad (1)$$

$$dc_2/dt = k_1'c_1 \quad (2)$$

$$dc_3/dt = k_2'c_1 - (k_3'+k_4')c_3 \quad (3)$$

$$dc_4/dt = k_3'c_3 \quad (4)$$

where c_1, c_2, c_3 and c_4 represent the concentrations of **1**, **2**, **3**, and **4**, respectively, and t is the time. These differential equations can be converted to the integral forms of Eqs. 5 to 8 by taking the Laplace transformation, where C_0 is the initial concentration of **1**, and $c_1(t)$, $c_2(t)$,

$$c_1(t) = C_0\left(\frac{\alpha+k_3'+k_4'}{\alpha-\beta}\right)e^{\alpha t} + C_0\left(-\frac{\beta+k_3'+k_4'}{\alpha-\beta}\right)e^{\beta t} \quad (5)$$

$$c_2(t) = C_0k_1\left[\left(-\frac{\alpha+k_3'+k_4'}{\alpha(\alpha-\beta)}\right) + \frac{\beta+k_3'+k_4'}{\beta(\alpha-\beta)} + \left(\frac{\alpha+k_3'+k_4'}{\alpha(\alpha-\beta)}\right)e^{\alpha t} - \left(\frac{\beta+k_3'+k_4'}{\beta(\alpha-\beta)}\right)e^{\beta t}\right] \quad (6)$$

$$c_3(t) = C_0k_2'\left(\frac{1}{\alpha-\beta}e^{\alpha t} - \frac{1}{\alpha-\beta}e^{\beta t}\right) \quad (7)$$

$$c_4(t) = \frac{C_0k_2'k_3'}{\alpha\beta(\alpha-\beta)}[(\alpha-\beta) + \beta e^{\alpha t} - \alpha e^{\beta t}] \quad (8)$$

$$\alpha \text{ and } \beta = \frac{-(k_1'+k_2'+k_3'+k_4') \pm \sqrt{(k_1'+k_2'+k_3'+k_4')^2 - 4(k_1'k_3'+k_1'k_4'+k_2'k_3')}}{2} \quad (\alpha \neq \beta) \quad (9)$$

$c_3(t)$ and $c_4(t)$ represent the concentrations of **1**, **2**, **3** and **4** at time t, respectively, and α and β are represented by Eq. 9.

By adapting the nonlinear least-squares method (MULTI)[4] to Eqs. 5 to 8 with the observed molar fractions of **1** and its degradation products, the rate constants, k_1', k_2', k_3', and k_4' were calculated at pH 8.88, 9.50 and 9.96 (Table II). Good agreement was observed between the experimental and calculated values, as shown in Fig. 3.

The relationship between the logarithmic value of these calculated rate constants and pH was linear, as shown in Fig. 4. The slopes were 1.0 for k_1', 0.9 for k_2', 0.9 for k_3' and 0.7 for k_4'. These results indicate that all the reactions shown in Chart 2 are catalyzed by hydroxide ion. As indicated in Table II, these reaction rates are in the order of $k_1' > k_3' > k_2' > k_4'$ at all the pH values studied, which indicates that the *S*-epimer, **1**, is more easily subject to both epimerization and β-lactam ring opening than the *R*-epimer, **3**. The lower stability of the *S*-epimer probably arises from the steric hindrance between the two groups at the C-2 and C-3

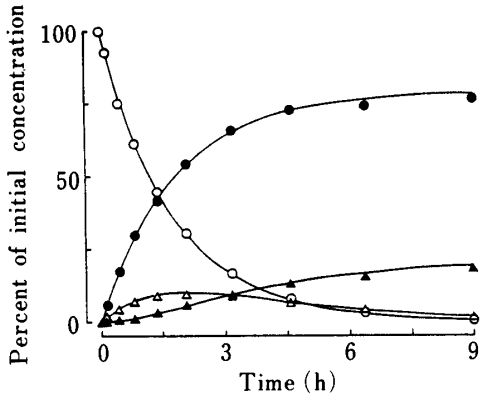

Fig. 3. Time Courses for Disappearance and Appearance of **1** and Its Degradation Products in Alkaline Solution (pH 9.50, $\mu=0.5$)

○, observed amount of **1**; ●, observed amount of **2**; △, observed amount of **3**; ▲, observed amount of **4**; ——, the least-squares fit of the experimental data.

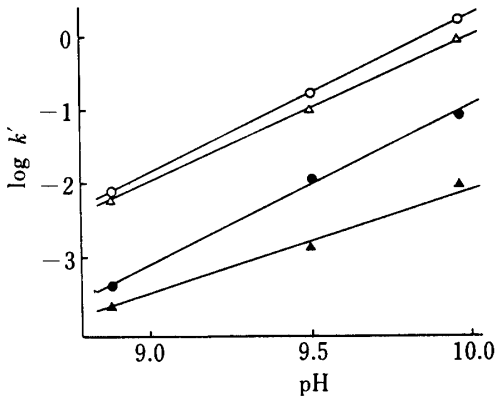

Fig. 4. Linear Correlation between Rate Constant and pH

○, experimental value of k_1'; ●, experimental value of k_2'; △, experimental value of k_3'; ▲, experimental value of k_4'; ——, linear regression fit of the experimental data.

TABLE II. Rate Constants for Epimerization and β-Lactam Ring-Opening Reaction of **1** in Alkaline Solution at 35 °C and $\mu=0.5$

pH	Rate constant (h^{-1})			
	k_1'	k_2'	k_3'	k_4'
8.88	0.12	0.033	0.11	0.025
9.50	0.45	0.14	0.36	0.055
9.96	1.23	0.33	0.95	0.13

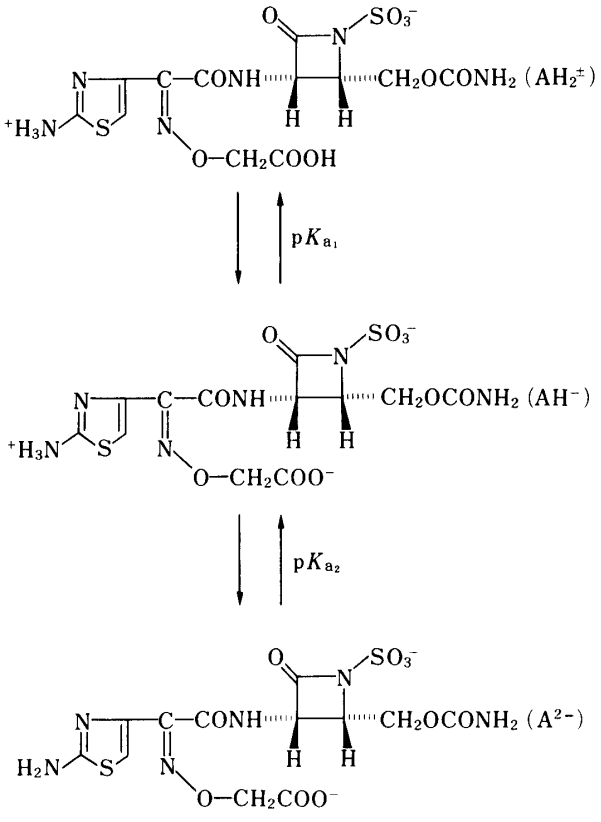

Chart 3

positions, which produces a strain on both the proton at the C-3 position and the β-lactam ring. Further support for this view came from the fact that the signal of the proton at the C-3 position of the *S*-epimer, **1** (5.32 ppm in DMSO-d_6), was shifted to lower field than that of *R*-epimer, **3** (4.84 ppm in DMSO-d_6), in the ^{1}H-NMR spectrum.

pK_a Determination

Compound **1** has three ionizing groups, the amino, carboxylic and sulfonyl groups. Generally the pK_a value of a sulfonyl group is very small,[5] and this group can be considered to dissociate in the pH range studied. The dissociation step of **1** is presented in Chart 3. Titration of the disodium salt of **1** with acid is a process of proton association from the dianion (A^{2-}) *via* the monoanion (AH^-) to the zwitterion ($AH_2^{\pm}$). The mixed dissociation constants K_1' and K_2' are defined by Eqs. 10 and 11,[3] where $[AH_2^{\pm}]$, $[AH^-]$ and $[A^{2-}]$ represent the molar concentrations of the zwitterion, monoanion, and dianion forms of **1**, γ_Z, γ_{MA} and γ_{DA} represent the activity coefficients of $AH_2^{\pm}$, AH^- and A^{2-}, respectively, $\{H^+\}$

represents the activity of the hydrogen ion, and K_1 and K_2 are the corresponding thermodynamic dissociation constants of **1**. In a solution with a total drug concentration of a mol, Eq. 12 holds, and when a strong monobasic acid is used for titration to give a molar concentration b, electroneutrality requires Eq. 13.[6]

$$K_1' = [AH^-]\{H^+\}/[AH_2^\pm] = K_1 \times \gamma_Z/\gamma_{MA} \quad (10)$$

$$K_2' = [A^{2-}]\{H^+\}/[AH^-] = K_2 \times \gamma_{MA}/\gamma_{DA} \quad (11)$$

$$a = [AH_2^\pm] + [AH^-] + [A^{2-}] \quad (12)$$

$$2a + [H^+] = [AH^-] + 2[A^{2-}] + [OH^-] + b \quad (13)$$

$$a = a_0 V/(V+x) \quad (14)$$

$$b = nV/(V+x) \quad (15)$$

$$x = V(a_0 C - AB - 2a_0 B)/(A-n)B \quad (16)$$

$$A = \{H^+\}/\gamma_\pm - K_w/\{H^+\}\gamma_\pm$$

$$B = \{H^+\}^2 + K_1'\{H^+\} + K_1'K_2' \quad (17)$$

$$C = K_1'\{H^+\} + 2K_1'K_2'$$

During the titration, a and b are expressed by Eqs. 14 and 15, respectively, where a_0, V, x and n represent the initial molar concentration of **1**, the initial volume, the titration volume, and the normality of the titrant, respectively. Equations 10 to 15 gave Eq. 16, in which A, B and C are defined by Eq. 17, where K_w is the dissociation constant of water (2.89×10^{-14} at 35 °C) and $\gamma_\pm$ is the mean activity constant (at 35 °C, 0.845 at $\mu = 0.2$, 0.762 at $\mu = 0.5$, 0.734 at $\mu = 0.8$).[7] By applying the nonlinear least-squares method (MULTI) to Eq. 16, K_1' and K_2' were obtained.

The mixed dissociation constants, pK_1' and pK_2', at 35 °C were 2.47 and 3.57 at $\mu = 0.2$, 2.44 and 3.56 at $\mu = 0.5$, and 2.46 and 3.57 at $\mu = 0.8$, respectively. Figure 5 shows the good agreement of the experimental data and the calculated titration curve at 35 °C and $\mu = 0.5$.

Catalytic Effect of Buffer Salts

The catalytic effect of the buffer salts used in the kinetic study was determined at constant

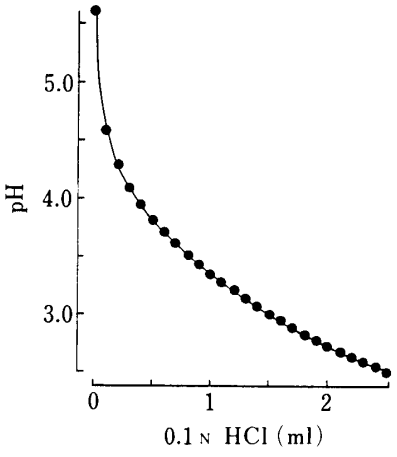

Fig. 5. Titration Curve for Carumonam Sodium with 0.1 N Hydrochloric Acid at 35 °C and $\mu = 0.5$

●, experimental value; ——, least-squares fit of the experimental data.

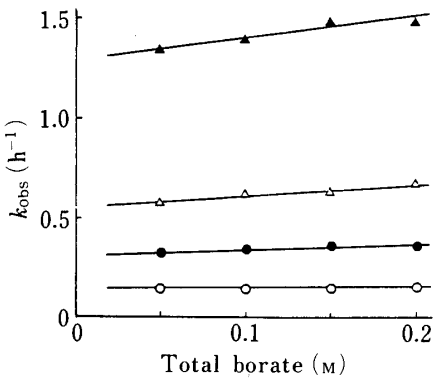

Fig. 6. Buffer Catalytic Effect on Degradation of **1** in Borate Buffer Solution at 35 °C and $\mu = 0.5$

○, pH 7.92; ●, pH 9.12; △, pH 9.50; ▲, pH 9.99.

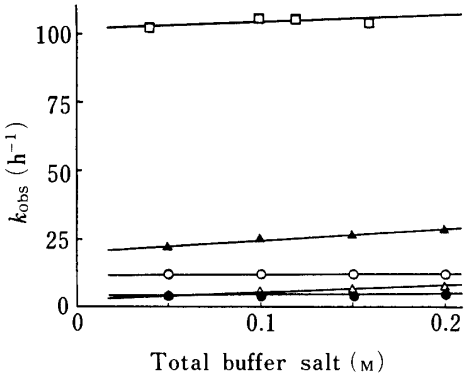

Fig. 7. Buffer Catalytic Effect on Degradation of **1** in Citrate, Acetate and Phosphate Buffer Solutions at 35 °C and $\mu=0.5$

○, citrate buffer (pH 2.75); ●, acetate buffer (pH 4.40); △, phosphate buffer (pH 5.84); ▲, phosphate buffer (pH 7.01); □, phosphate buffer (pH 7.82).

$$AH_2^{\pm} + H^+ \longrightarrow P \quad k_1$$
$$AH^- + H^+ \longrightarrow P \quad k_2$$
$$AH^- \xrightarrow{H_2O} P \quad k_3$$
$$A^{2-} + OH^- \longrightarrow P \quad k_4$$
$$A^{2-} \xrightarrow{H_2O} P \quad k_5$$

Chart 4

Table III. Rate Constants for Degradation of **1** in Aqueous Solutions at 35 °C and $\mu=0.5$

k_1	0.0035	$h^{-1}\,mol^{-1}$
k_2	0.076	$h^{-1}\,mol^{-1}$
k_3	0.0017	h^{-1}
k_4	5520	$h^{-1}\,mol^{-1}$
k_5	0.00023	h^{-1}

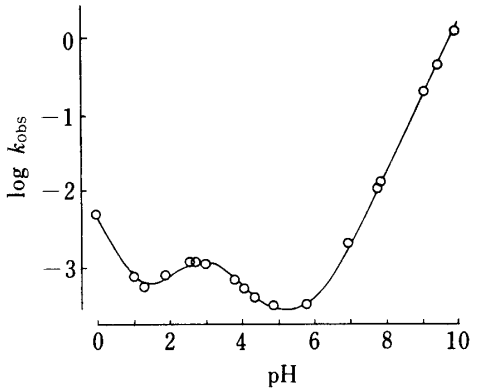

Fig. 8. log k_{obs}–pH Profile for Degradation of **1** in Aqueous Solution at 35 °C and $\mu=0.5$

○, experimental value; ——, theoretical curve calculated from Eq. 20.

pH, temperature (35 °C), ionic strength ($\mu=0.5$) and drug concentration, with only the buffer concentration being varied from 0.05 to 0.2 M. This experiment was done at several pH values within the effective range for each buffer employed. The catalytic effect was observed in phosphate and borate buffers as shown in Figs. 6 and 7, and the rate constants, which were purely dependent on pH, were obtained by extrapolation to zero buffer concentration. No appreciable effect on the degradation of **1** was observed with citrate and acetate buffers as shown in Fig. 7. The pseudo-first-order rate constants, which were considered as buffer-free, are given in Table I.

pH-Rate Profile

The pH-rate profile for the degradation of **1** showed a unique W-shape having the characteristic maximum at pH 2.8 and minimum in the pH range of 4.9 to 5.8, as shown in Fig. 8. There are at least five reactions which contribute to the overall velocity for the degradation of **1** in aqueous solution. They are shown in Chart 4, with k_1, k_2, k_3, k_4 and k_5 being the corresponding reaction rate constants. The overall velocity (v) is obviously equal to the sum of the rates of these reactions as given in the following equations (Eqs. 18 and 19).[8]

$$v=k_1[AH_2^{\pm}][H^+]+k_2[AH^-][H^+]+k_3[AH^-] + k_4[A^{2-}][OH^-]+k_5[A^{2-}] \quad (18)$$

$$v=k_{obs}([AH_2^{\pm}]+[AH^-]+[A^{2-}]) \quad (19)$$

Introducing Eqs. 10 and 11 into these two equations gave Eq. 20, which expresses the correlation between pH and the pseudo-first-order constant.

$$k_{obs}=\frac{k_1\{H^+\}^3+k_2K'_1\{H^+\}^2+k_3K'_1\{H^+\}\gamma_{\pm}+k_4K'_1K'_2K_w/\{H^+\}+k_5K'_1K'_2\gamma_{\pm}}{(\{H^+\}^2+K'_1\{H^+\}+K'_1K'_2)\gamma_{\pm}} \quad (20)$$

By applying the nonlinear least-squares method (MULTI) to the experimental data, k_1 to k_5 were obtained (Table III). In Fig. 8, the solid line represents the theoretical curve and the solid circles are the experimental data. The good agreement indicates that the hypothesis regarding the degradation pattern of **1** is reasonable. From the calculated rate constants, the maximum of the W-shaped pH-rate profile is due to solvolysis of the monoanion in Chart 4; the main degradation product is **7**. This indicates that the monoanion form of **1** (AH^-) easily isomerizes to the *E*-isomer (**7**) around pH 2.8.

Primary Salt Effect

The primary salt effect on the degradation of **1** was studied at constant pH and temperature, while varying the ionic strength by addition of sodium chloride. Studies were conducted at pH 1.06, 3.04, 4.08 and 9.57, where general base catalysis was absent or negligible. The logarithmic values of reaction rates at $\mu=0.2$, 0.5 and 0.8 at constant pH are given in Table IV. As shown in Fig. 9, a positive salt effect at pH 9.57 and slight negative salt effects at pH 1.06, 3.04, and 4.08 were observed.

When species A and B react in high ionic strength solution, Eq. 21 gives the correlation between rate constant and ionic strength, where Q is constant at constant temperature and is 1.036 at 35 °C, and Z_A and Z_B are the charges of reaction species A and B, respectively.[9]

TABLE IV. First-Order Rate Constants for Degradation of **1** at Several pH Values and Ionic Strengths at 35 °C

pH	μ	Observed log k	Calculated log k
1.06	0.2	−3.06	−3.10
	0.5	−3.10	−3.10
	0.8	−3.14	−3.12
3.04	0.2	−2.95	−2.92
	0.5	−2.95	−2.92
	0.8	−2.96	−2.93
4.08	0.2	−3.24	−3.24
	0.5	−3.28	−3.24
	0.8	−3.28	−3.24
9.57	0.2	−0.40	−0.51
	0.5	−0.21	−0.25
	0.8	−0.12	−0.11

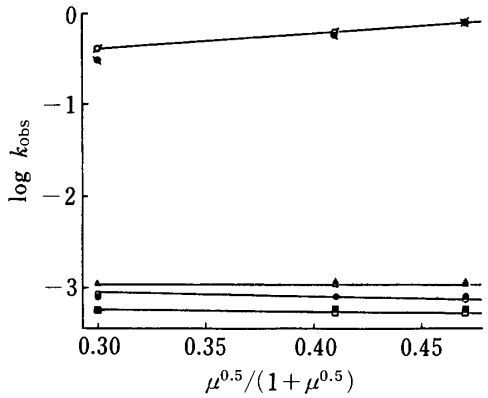

Fig. 9. Effect of Ionic Strength on Pseudo-First-Order Rate Constant

○, experimental value at pH 1.06; △, experimental value at pH 3.04; □, experimental value at pH 4.08; ◇, experimental value at pH 9.57; ●, calculated value at pH 1.06; ▲, calculated value at pH 3.04; ■, calculated value at pH 4.08; ◆, calculated value at pH 9.57.

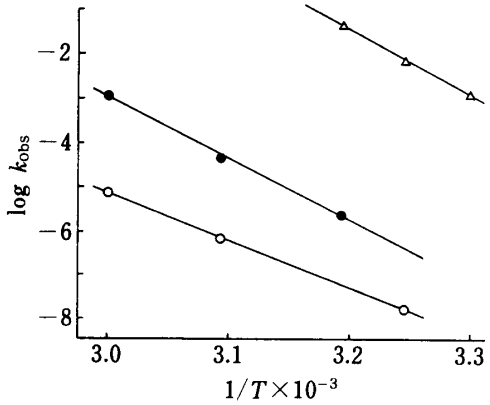

Fig. 10. Arrhenius Plots for Degradation of **1** at Several pH Values and $\mu=0.5$

○, pH 4.40; ●, pH 7.01; △, pH 8.88.

Equation 21 should hold for each of the reactions cited in Chart 4, and the reaction rate constants k_1, k_2, k_3, k_4, and k_5 are given by Eqs. 22 to 26,

$$\log k = \log k^\circ + 2QZ_AZ_B\mu^{0.5}/(1+\mu^{0.5}) \quad (21)$$

$$k_1 = k_1^\circ \quad (22)$$

$$k_2 = k_2^\circ \times 10^{-2QI} \quad (23)$$

$$k_3 = k_3^\circ \quad (24)$$

$$k_4 = k_4^\circ \times 10^{4QI} \quad (25)$$

$$k_5 = k_5^\circ \quad (26)$$

$$(I = \mu^{0.5}/(1+\mu^{0.5}))$$

where k_1°, k_2°, k_3°, k_4°, and k_5° are the reaction rate constants at zero ionic strength. Equations 22 to 26 and 20 gave Eq. 27, which presents the relationship between the pseudo-first-order reaction rate and the ionic strength. Figure 9 and Table IV show reasonable agreement

$$k_{obs} = \frac{k_1^\circ\{H^+\}^3 + k_2^\circ K_1'\{H^+\}^2 10^{-2QI} + k_3^\circ K_1'\{H^+\}\gamma_\pm + k_4^\circ K_1'K_2'K_w 10^{4QI}/\{H^+\} + k_5^\circ K_1'K_2'\gamma_\pm}{(\{H^+\}^2 + K_1'\{H^+\} + K_1'K_2')\gamma_\pm} \quad (27)$$

between plots of $\log k$ *versus* $\mu^{0.5}/(1+\mu^{0.5})$ from the experimental data and the calculated results from Eq. 27. Thus, the kinetic salt effect could be well explained by considering all the reaction processes which occur simultaneously.

Effect of Temperature

The temperature dependence of the degradation of **1** was determined by measuring the pseudo-first-order reaction rate constants at several temperatures and $\mu=0.5$ in 0.1 M total buffer salt. The apparent activation energies of **1**, calculated from the slopes of the Arrhenius plots shown in Fig. 10, were 22.3, 28.7 and 30.6 kcal/mol at pH 4.40, 7.01 and 8.88, respectively. With 13.1 kcal/mol as the heat of water,[7] the values of activation energy of **1** at pH 7.01 and 8.88 were 15.6 and 17.5 kcal/mol, respectively. The activation energies for the degradation of **1** are similar to those of penicillins and cephalosporins.[10]

Acknowledgements We are grateful to Drs. K. Morita, T. Maruyama and M. Ochiai of this division for their encouragement throughout this work.

References

1) A. Imada, K. Kitano, K. Kintaka, M. Muroi, and M. Asai, *Nature* (London), **289**, 590 (1981).
2) *a*) S. Kishimoto, M. Sendai, S. Hashiguchi, M. Tomimoto, Y. Satoh, T. Matsuo, M. Kondo, and M. Ochiai, *J. Antibiot.*, **36**, 1421 (1983); S. Kishimoto, M. Sendai, M. Tomimoto, S. Hashiguchi, T. Matsuo, and M. Ochiai, *Chem. Pharm. Bull.*, **32**, 2646 (1984); *b*) M. Sendai, S. Hashiguchi, M. Tomimoto, S. Kishimoto, T. Matsuo, M. Kondo, and M. Ochiai, *J. Antibiot.*, **38**, 346 (1985); M. Sendai, S. Hashiguchi, M. Tomimoto, S. Kishimoto, T. Matsuo, and M. Ochiai, *Chem. Pharm. Bull.*, **33**, 3798 (1985).
3) A. Albert and E. P. Serjeant, "The Determination of Ionization Constants," 3rd ed., Chapman and Hall, London, 1984, pp. 47—60.
4) K. Yamaoka, Y. Tanigawara, T. Nakagawa, and T. Uno, *J. Pharmacobio-Dyn.*, **4**, 879 (1981).
5) C. H. Rochester, "Acidity Functions," Academic Press, London, 1970, pp. 96—100.
6) J. C. Speakman, *J. Chem. Soc.*, **1940**, 855; D. Litchinsky, N. Purdie, M. B. Tomson, and W. D. White, *Anal. Chem.*, **41**, 1726 (1969).
7) H. S. Harned and W. J. Hammer, *J. Am. Chem. Soc.*, **55**, 2194 (1933).
8) J. P. Hou and J. W. Poole, *J. Pharm. Sci.*, **58**, 447 (1969).
9) J. T. Carstensen, *J. Pharm. Sci.*, **59**, 1140 (1970); E. R. Garrett, J. T. Bojarski, and G. J. Yakatan, *ibid.*, **60**, 1145

(1971).
10) T. Yamana, A. Tsuji, and Y. Mizukami, *Chem. Pharm. Bull.*, **22**, 1186 (1974); T. Yamana and A. Tsuji, *J. Pharm. Sci.*, **65**, 1563 (1976); E. S. Rattie, J. J. Zimmerman, and L. J. Ravin, *ibid.*, **68**, 1369 (1979); A. Tsuji, E. Nakashima, Y. Deguchi, K. Nishide, T. Simizu, S. Horiuchi, K. Ishikawa, and T. Yamana, *ibid.*, **70**, 1120 (1981); T. Fujita, Y. Harima, and A. Koshiro, *Chem. Pharm. Bull.*, **31**, 2103 (1983); H. Fabre, N. H. Eddine, and G. Berge, *J. Pharm. Sci.*, **73**, 611 (1984).